

Composition-dependent mechanism of formation of $\gamma\text{-Fe}_2\text{O}_3$ /carboxymethylcellulose nanocomposites

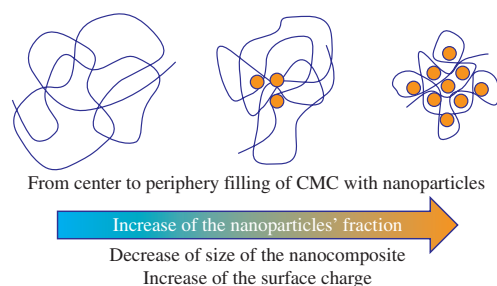
Ekaterina E. Yurmanova, Irina M. Le-Deygen, Vasily V. Spiridonov and Andrey V. Sybachin*

Department of Chemistry, M. V. Lomonosov Moscow State University, 119991 Moscow, Russian Federation.

Fax: +7 495 939 0174; e-mail: sybachin@mail.ru

DOI: 10.1016/j.mencom.2020.11.026

The distribution of nanoparticles in the volume of the composite is determined by a ratio between reagents at the stage of synthesis. At low molar fractions of iron in the system, nanoparticles are formed inside the coils of macromolecules, and nanoparticles expand their formation closer to the surface with an increase in the iron fraction. The size of the nanoparticles remains independent of the polymer/iron ratio in the reaction mixture.



Keywords: nanocomposite, iron oxide, maghemite, carboxymethylcellulose, nanoparticles.

Composite materials based on polymers and metal nanoparticles are of biomedical interest.^{1,2} A polymer matrix provides strength, mechanical and adhesive properties of the material, while nanoparticles give additional biocide, catalytic and magnetic properties.^{3–5} In creating these materials, it is important to obtain a uniform distribution of nanoparticles in the matrix. First, the mechanical dispersion of prepared nanoparticles in the polymer matrix can be used.^{6,7} This process can be accompanied by the mechanical damaging of polymers, additional aggregation of nanoparticles, uncontrollable distribution of the nanoparticles in the volume of polymers, etc. Second, the direct synthesis of nanoparticles in the presence of a polymer matrix can be performed.^{8,9} Polymers can organize centers for the growth of nanoparticles, sterically restrict it, and stabilize nanoparticles with charged groups. It was found earlier that carboxymethylcellulose (CMC) can serve as a matrix for $\gamma\text{-Fe}_2\text{O}_3$ (maghemite) nanoparticles in one-pot synthesis.¹⁰

The magnetic nanoparticles of magnetite and maghemite are the most widespread forms of iron oxides.¹¹ The aim of this work was to study the distribution of $\gamma\text{-Fe}_2\text{O}_3$ nanoparticles upon synthesis in a CMC polymer matrix depending on the fraction of iron in an initial mixture and the physicochemical properties of the resulting nanocomposites.

The composites were prepared by synthesizing iron oxide nanoparticles in a solution of CMC sodium salt (Na–CMC) with a molecular weight of 90000 using Mohr's salt as a precursor.¹⁰ The nanocomposites were obtained by the treatment of an alkaline solution of Mohr's salt with sodium hypophosphite in the presence of Na–CMC at room temperature. The reaction was carried out in air since oxygen is required to produce the oxidized form of iron. The obtained samples and Na–CMC were dialyzed against twice distilled water.

The molar ratio (μ) between the monomer units of the polysaccharide and Fe^{2+} ions in the synthesis was varied from 0.04 to 1. The polysaccharide concentration was 2 wt%. Note that only water-soluble products were formed with the above concentrations and amounts of reagents. As a result, three

$\gamma\text{-Fe}_2\text{O}_3$ /Na–CMC nanocomposites, in which the brown color intensity increased with the iron content of the system, were obtained (see details in Online Supplementary Materials).

The sizes of the nanocomposites were evaluated by quasi-elastic laser light scattering. The diameter of pure Na–CMC in a Tris buffer with pH 7 was 285 nm. Incorporation of $\gamma\text{-Fe}_2\text{O}_3$ nanoparticles in a Na–CMC matrix with $\mu = 0.04$ (composite I) resulted in a decrease of the mean diameter to 115 nm. A further increase in the fraction of nanoparticles in a Na–CMC matrix with $\mu = 0.25$ (composite II) resulted in a decrease of the mean size to 95 nm. Finally, for the nanocomposite with $\mu = 1$ (composite III), the mean diameter was 85 nm. This contraction can be attributed to the action of $\gamma\text{-Fe}_2\text{O}_3$ nanoparticles as inter-macromolecular cross-linking agents. Nevertheless, this size measurement cannot elucidate the overall distribution of nanoparticles within Na–CMC macromolecules.

The electrophoretic mobility (EPM) of the nanocomposites was measured to evaluate the surface charges of particles (Figure 1). The EPM value of composite I was $-1.5 \mu\text{m cm s}^{-1} \text{V}^{-1}$, which is equal to the value for pure Na–CMC. An increase in the fraction of nanoparticles in the nanocomposites raised the overall negative EPM values to $-2.5 \mu\text{m cm s}^{-1} \text{V}^{-1}$ for composite II and

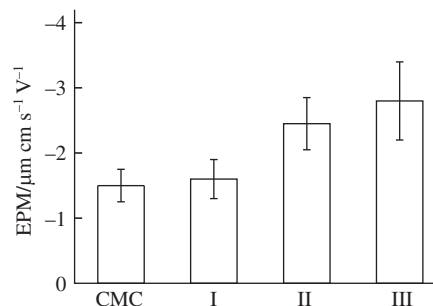


Figure 1 EPM of pure Na–CMC and composites I–III (Tris buffer solution with pH 7.0; concentration of macromolecules, 0.5 mg ml⁻¹).

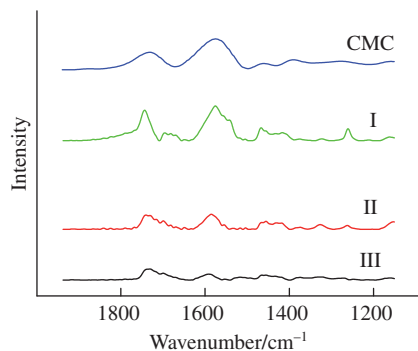


Figure 2 IR spectra of nanocomposites I–III (Tris buffer, pH 7.0; concentration of macromolecules, 0.5 mg ml⁻¹).

–2.8 $\mu\text{m cm s}^{-1} \text{V}^{-1}$ for composite III. This result seems unexpected. The surface charge of maghemite nanoparticles can vary in a wide range from completely positive at pH below 3.5 to completely negative at pH above 10 with an isoelectric point in a range of pH 6.9–7.5.^{12,13} At pH 7, an expected ζ -potential value of nanoparticles is close to zero. One could anticipate no or negligible influence of nanoparticles on the EPM of Na–CMC composites; however, the observed results indicated a contrast behavior. The following explanation can be proposed. It is well known that the complexation of weak polyanions with oppositely charged macromolecules induces additional deprotonation of functional groups.¹⁴ The same situation should be expected for $\gamma\text{-Fe}_2\text{O}_3$ nanoparticles due to the effect of positively charged surface groups of maghemite.

The IR spectra of the samples were measured in a Tris buffer solution with pH 7 to control the equilibrium of carboxyl/carboxylate groups in the composites (Figure 2). Composite I exhibited an intense sharp peak at 1750 cm^{-1} due to the vibration of protonated carboxyl groups, a broad peak at 1690 cm^{-1} due to the vibration of carbonyl group, and a sharp peak at 1580 cm^{-1} and a doublet at 1420 and 1460 cm^{-1} due to the vibration of deprotonated carboxylate groups.¹⁵ In a solution of pure Na–CMC, the broad peaks of protonated carboxyl and carbonyl groups overlapped due to numerous internal hydrogen bonds between them.¹⁶ An increase in the intensity ratio between carboxylate and carboxyl peaks was observed for composites II and III to indicate a shift of equilibrium towards charged forms. As the number of oxide nanoparticles in the sample was increased, a noticeable vanishing of the peak of stretching vibrations of the double bond C=O was observed.¹⁵ This effect can be attributed to negative charge delocalization between the oxygen atoms of a carboxyl group.¹⁰

Note that the data of EPM measurements correspond to the surface charge of the particle. A growth in the overall negative surface charge of the nanocomposites corresponds to an increase in the number of the uncompensated deprotonated carboxylate groups. Thus, we concluded that nanoparticles are situated inside the macromolecular coil of Na–CMC rather than on the surface. Due to a low negative surface charge of composite I, positively charged nanoparticles are settled far from the surface deep close to the centre of macromolecule. The distance between nanoparticles and the surface is long enough to prevent the charging of surface carboxyl groups. With a low ratio of iron to carboxyl groups in the reaction mixture, the stabilization of $\gamma\text{-Fe}_2\text{O}_3$ nanoparticles

with Na–CMC results in the formation of a nanocomposite with the nanoparticles situated close to the centre. An increase in the fraction of iron in the reaction mixture results in the filling of the internal nanocomposite volume with nanoparticles from centre to the surface. The statistical distribution of the nanoparticles distributed from the centre to the periphery of the nanocomposite. This finding provides an opportunity to organize the directed synthesis of nanocomposites with adjustable size, charge, and spatial distribution of nanoparticles.

Thus, the nanocomposites of Na–CMC with $\gamma\text{-Fe}_2\text{O}_3$ nanoparticles with different iron contents were obtained by a direct one-pot synthesis. With increasing the iron content, the nanoparticles distributed from the centre to the periphery of the nanocomposite. This finding provides an opportunity to organize the directed synthesis of nanocomposites with adjustable size, charge, and spatial distribution of nanoparticles.

This work was supported by the Russian Foundation for Basic Research (project no. 18-03-01024).

Online Supplementary Materials

Supplementary data associated with this article can be found in the online version at doi: 10.1016/j.mencom.2020.11.026.

References

- J. Yu, Y. Rong, C.-T. Kuo, X.-H. Zhou and D. T. Chiu, *Anal. Chem.*, 2017, **89**, 42.
- J. Hu, Y. Sheng, J. Shi, B. Yu, Z. Yu and G. Liao, *Curr. Drug Metab.*, 2018, **19**, 723.
- M. A. Morsi and A. E. M. Hezma, *J. Mater. Res. Technol.*, 2019, **8**, 2098.
- L. Tamayo, M. Azócar, M. Kogan, A. Riveros and M. Páez, *Mater. Sci. Eng., C*, 2016, **69**, 1391.
- M. N. Efimov, A. A. Vasilev, E. V. Chernikova, R. V. Toms, D. G. Muratov, G. V. Pankina, P. A. Chernavskii and G. P. Karpacheva, *Mendeleev Commun.*, 2018, **28**, 556.
- M. Mauer, P. Kalenda, M. Honne and P. Vacikova, *J. Phys. Chem. Solids*, 2012, **73**, 1150.
- J. Jampilek and K. Král'ová, in *Nanostructures for Antimicrobial Therapy*, eds. A. Ficaí and A. M. Grumezescu, Elsevier, 2017, pp. 23–54.
- S. P. Gubin, E. M. Moroz, A. I. Boronin, V. V. Kriventsov, D. A. Zyuzin, N. A. Popova, E. K. Florina and A. M. Tsirlin, *Mendeleev Commun.*, 1999, **9**, 59.
- A. A. Zezin, A. I. Emel'yanov, G. F. Prozorova, E. A. Zezina, V. I. Feldman, S. S. Abramchuk and A. S. Pozdnyakov, *Mendeleev Commun.*, 2019, **29**, 158.
- V. V. Spiridonov, I. G. Panova, L. A. Makarova, M. I. Afanasov, S. B. Zezin, A. V. Sybachin and A. A. Yaroslavov, *Carbohydr. Polym.*, 2017, **177**, 269.
- A. M. Dentin, T. G. Khonina, E. V. Shadrina, E. A. Bogdanova, D. K. Kuznetsov, A. V. Mekhaev, V. Ya. Shur and V. P. Krasnov, *Russ. Chem. Bull., Int. Ed.*, 2019, **68**, 1178 (*Izv. Akad. Nauk, Ser. Khim.*, 2019, 1178).
- I. T. Lucas, S. Durand-Vidal, E. Dubois, J. Chevalet and P. Turq, *J. Phys. Chem. C*, 2007, **111**, 18568.
- M. Kosmulski, *Adv. Colloid Interface Sci.*, 2020, **275**, 102064.
- V. A. Kabanov, *Russ. Chem. Rev.*, 2005, **74**, 3 (*Usp. Khim.*, 2005, **74**, 5).
- E. Pretsch, P. Bühlmann and C. Affolter, *Structure Determination of Organic Compounds: Tables of Spectral Data*, Springer, Berlin, Heidelberg, 2000.
- S. Rózańska and J. Rózański, *Soft Mater.*, 2017, **15**, 302.

Received: 22nd July 2020; Com. 20/6270